Available online at www.sciencedirect.com
ScienceDirect
Developmental Biology 298 (2006) 312–326
DEVELOPMENTAL BIOLOGY
www.elsevier.com/locate/ydbio

Xenopus Teashirt1 regulates posterior identity in brain and cranial neural crest

Katja Koebernick [a], Jubin Kashef [b], Tomas Pieler [a], Doris Wedlich [b,*]

[a] *Institute of Biochemistry, University of Goettingen, Justus-von-Liebig-Weg 11, 37077 Goettingen, Germany*
[b] *Institute of Zoology II, University of Karlsruhe, Fritz-Haber-Weg 4, 76131 Karlsruhe, Germany*

Received for publication 30 November 2005; revised 20 June 2006; accepted 26 June 2006
Available online 30 June 2006

Abstract

We have isolated two related *Xenopus* homologues of the homeotic zinc finger protein Teashirt1 (Tsh1), XTsh1a and XTsh1b. While *Drosophila* teashirt specifies trunk identity in the fly, the developmental relevance of vertebrate Tsh homologues is unknown. XTsh1a/b are expressed in prospective trunk CNS throughout early neurula stages and later in the migrating cranial neural crest (CNC) of the third arch. In postmigratory CNC, XTsh1a/b is uniformly activated in the posterior arches. Gain- and loss-of-function experiments reveal that reduction or increase of XTsh1 levels selectively inhibits specification of the hindbrain and mid/hindbrain boundary in *Xenopus* embryos. In addition, both overexpression and depletion of XTsh1 interfere with the determination of CNC segment identity. In transplantation assays, ectopic XTsh1a inhibits the routing of posterior, but not of mandibular CNC streams. The loss of function phenotype could be rescued with low amounts either of XTsh1a or murine Tsh3. Our results demonstrate that proper expression of XTsh1 is essential for segmentally restricted gene expression in the posterior brain and CNC and suggest for the first time that teashirt genes act as positional factors also in vertebrate development.

Keywords: Teashirt; *Xenopus*; Cranial neural crest; Zinc finger; Hindbrain; Cell migration; Hox; Ephrin; Branchial arches

Introduction

The cranial neural crest (CNC) is a migratory population of cells, which gives rise to a great variety of different cell types in the vertebrate head, including cartilage and bones of the face and jaw, as well as peripheral neurons, glia and pigment cells (reviewed in Santagati and Rijli, 2003). Prior to neurulation, CNC cells are specified at the lateral margins of the anterior neural plate bordering the prospective non-neural ectoderm. They initiate migration by detaching from the dorsal neural tube or the closing neural folds and colonize ventrolateral regions of the embryo following stereotypical routes. In *Xenopus*, three major populations of migrating CNC cells originate at distinct axial levels of the mid- and hindbrain and target the mandibular (first), hyoid (second) and two distinct branchial (third and fourth) arches, respectively (Sadaghiani and Thiébaud, 1987). Derivatives of the first two arches contribute to the facial bones, while CNC of the third and the fourth arches differentiates into gill cartilage.

The segmental organization of the CNC is preceded by the subdivision of its major source, the hindbrain, into rhombomeric units. Transplantation studies in the chicken established that each individual CNC stream is populated from a defined group of rhombomeres and is hallmarked either by a lack of Hox gene expression in anterior CNC or the expression of a distinct set of Hox genes in posterior CNC (Lumsden et al., 1991; Hunt and Krumlauf, 1991; Hunt et al., 1991; Prince and Lumsden, 1994). Although evidence from several grafting experiments suggested that the developmental fate of CNC cells is prespecified ahead of migration by positional cues of the anteroposterior (AP) axis, more recent transplantation studies also revealed plasticity in the differentiation potential of CNC cells (Noden, 1993, reviewed in Trainor and Krumlauf, 2000a, b; Trainor et al., 2002). Thus, the segmental fates of CNC cells appear to be controlled both by regionalized, autonomous

* Corresponding author. Fax: +49 721 6083992.
E-mail address: doris.wedlich@zi2.uni-karlsruhe.de (D. Wedlich).

0012-1606/$ - see front matter © 2006 Elsevier Inc. All rights reserved.
doi:10.1016/j.ydbio.2006.06.041

factors in the brain and external factors acting on CNC cells in the pharyngeal arch target tissues.

Segment-specific changes in the adhesive properties of CNC cells and surrounding tissues coordinate the targeting of each individual CNC stream to its destination within the cranial mesenchyme. Even though the mechanisms of CNC guidance are still largely unclear, this process apparently requires the presence of CNC-repelling factors in specific zones of the paraxial mesoderm, particularly those located adjacent to r3 and r5 (Farlie et al., 1999). In the mouse, the receptor tyrosine kinase ErbB4 is involved in the establishment of a CNC-free zone in r3-adjacent mesenchyme (Golding et al., 2000). Collapsin-1/Semaphorin-III, another protein expressed in regions avoided by neural crest (NC) cells, appears to act as repulsive factor during the pathfinding of trunk and hindbrain NC in the chicken (Eickholt et al., 1999). Components of the ephrin signaling pathway have also been implicated in repulsive cell interactions controlling guidance during diverse migratory processes (Flanagan and Vanderhaeghen, 1998; Holder and Klein, 1999). Suggesting the involvement of ephrin signaling in NC routing, application of ephrin-B1 ligand to trunk explants of chicken embryos results in the misguidance of trunk neural crest cells (Krull et al., 1997). Ephrin-B2 was found to exert a similar inhibitory effect on trunk NC migration in the rat (Wang and Anderson, 1997). In *Xenopus*, the restricted expression of ephrin receptors and ligands in defined complementary segments of the hindbrain and neural crest was found to be crucial to delimit the segmental boundaries of CNC streams of the third and second and the third and fourth arch, respectively (Smith et al., 1997; Helbling et al., 1998).

In order to relocate, CNC cells need to interact with and actively remodel the extracellular matrix of the mesenchyme within their migration trails. Interestingly, pathfinding of the hyoid and branchial, but not the mandibular CNC, was revealed to depend on the activity of the metalloprotease ADAM 13 in *Xenopus* (Alfandari et al., 2001). This might indicate that CNC pathfinding in mandibular vs. hyoid/branchial CNC streams is regulated by discrete mechanisms. However, it remains to be established, which segmental determinants mediate the competence of individual CNC streams to target specific migration pathways and if homeotic factors are involved.

We have previously characterized the function of Xcadherin-11 (Xcad-11), a cell adhesion molecule expressed by emigrating CNC cells (Borchers et al., 2001). Using a CNC transplantation assay (Borchers et al., 2000), we could demonstrate that Xcad-11 regulates the velocity of CNC migration by modulating cellular adhesiveness.

Here, we report on the isolation and functional characterization of *Xenopus* Teashirt1 (XTsh1), a putative transcription factor expressed in migrating CNC cells in *Xenopus*. The homeotic zinc finger protein Teashirt (Tsh) was first identified in *Drosophila*, where it was characterized as a region-specific factor essential for the specification of segmental identities in the trunk (Fasano et al., 1991; Röder et al., 1992; DeZulueta et al., 1994). In addition, it was shown that *Drosophila* Tsh (DTsh) is required for the transcriptional repression of Ultrabithorax (Ubx) in the *Drosophila* midgut mesoderm, acting in concert with the transcriptional co-repressors C-terminal Binding Protein (CtBP) and Brinker (Brk) (Waltzer et al., 2001; Saller et al., 2002). In vertebrates, three Tsh homologues could be identified (Caubit et al., 2000; Manfroid et al., 2004), but their function during embryogenesis is as yet unknown. However, ectopic expression of all three murine Tsh genes (mTsh1/2/3) in *Drosophila* was reported to produce effects similar to those generated by DTsh (Manfroid et al., 2004), e.g. to induce head-to-trunk transformations in different head segments. Further suggesting a functional conservation of these proteins from flies to vertebrates, murine Tsh proteins were demonstrated to act as transcriptional repressors (Manfroid et al., 2004). Their spatial expression could be detected in the trunk region of the CNS apart from a small distal expression field in the branchial arches 1 and 2 around stage 11 d.p.c. (Caubit et al., 2000).

In the present study, we show that XTsh1 expression is also confined to the trunk region of the CNS in early *Xenopus* embryos, suggesting its possible role in segmental patterning of the CNS. Apart from this, we find that XTsh1 is expressed in emigrating CNC cells of the third arch and later the entire branchial arch region, implying a further function of XTsh1 in CNC development.

To address the relevance of XTsh1 during embryonic pattern formation, we performed gain- and loss-of-function analyses by microinjection of XTsh1a mRNA or XTsh1 antisense morpholino oligonucleotides (MO) into early cleavage stages. We find that ectopic expression of XTsh1 in *Xenopus* strongly interferes with the specification of mid- and hindbrain in early neurula stages, while more posterior and anterior levels of the CNS are not or less affected. Notably, these effects on early AP patterning are also produced by XTsh1-MO injection. NC induction could proceed normally in embryos injected with XTsh1a mRNA or XTsh1-MO. However, the segmentation pattern of CNC cells was severely disorganized during later embryonic stages. Moreover, the posterior arches did not acquire their proper identities in embryos overexpressing XTsh1a. CNC transplants from XTsh1a mRNA-injected embryos failed to colonize the posterior arches but were still capable to invade the mandibular arch region. Taken together, our data thus support two distinct functions of XTsh1 during embryogenesis; one in determining positional AP cues of the neuraxis and another in controlling segmental migration of CNC cells.

Materials and methods

Isolation of Teashirt1 homologues from Xenopus

Based on the human and murine Tsh protein sequences, degenerate primers were designed to amplify a Tsh cDNA fragment spanning the predicted zinc finger regions 2 and 3 (Tsh_deg_1F; 5′ TSA SYR YCC ACA TGA WVR AVA SMA ARC CAT, Tsh_deg_1R; 5′ CCA CAY YSC ATR CAC TTD ARK ATY TG). In an RT-PCR reaction using these primers, we obtained two different 312 bp fragments from stage 36 *Xenopus* cDNA revealing closest homology to the Teashirt1 protein. By means of 5′/3′ RACE RT-PCR (SMART RACE cDNA amplification kit, Clontech), overlapping fragments of the *Xenopus* Tsh1 (XTsh1) cDNAs could be identified and assembled to obtain the full coding sequences. Upon “end-to-end” RT-PCR on stage 36 *Xenopus* embryonic total

RNA, two distinct full-length cDNAs of 3.5 kb could be amplified and were termed XTsh1a and XTsh1b (GenBank accession nos. AY854806 and AY854807). For mRNA injection experiments, the entire ORF of XTsh1a was subcloned into the 5′ *Eco*RI/3′ *Xho*I sites of either pCS2+ or pCS2+MT to produce untagged or C-terminally myc-tagged XTsh1a protein, respectively.

XTsh1 antisense morpholino oligonucleotide design and analysis

Further 92 nucleotides of 5′UTR sequence were isolated by 5′ RACE using the oligonucleotide XTsh1b-1R (5′-CGGTGTACCAGGATCAGATGTTG-GACCACTT) and found to be identical for XTsh1a and XTsh1b. The functionality of an antisense morpholino oligonucleotide (GeneTools) targeting part of the XTsh1 5′UTR (XTsh1-MO: 5′-GGCTTCCGCAGGGCTTCTC-CACTCC) was tested by *in vitro* translation (TNT® Coupled Reticulocyte Lysate System, Promega) from an expression plasmid containing the 5′UTR and ORF of XTsh1a (pCS2+XTsh1a-5′UTR+ORF). Reactions (total volume 12.5 μl) containing undiluted and diluted MO oligonucleotides in a volume of 1 μl (stock concentration 1 mM) were carried out in the presence of ^{35}S-labeled methionine (Amersham). The standard control morpholino oligonucleotide (Co-MO, GeneTools) was used as negative control. An aliquot (5 μl) of each reaction was loaded on an 8% polyacrylamide gel, and proteins were visualized by SDS-PAGE and autoradiography.

Embryo generation, microinjection and in situ hybridization

Wild-type and albino *Xenopus* embryos were obtained by in vitro fertilization and cultivated following standard procedures. To synthesize capped mRNA, the template DNAs (pCS2+/XTsh1a or pCS2+MT/XTsh1a) were linearized with *Not*I and transcribed in vitro with the SP6 message machine kit (Ambion). XTsh1a mRNA or XTsh1-MO was injected in a volume of 5 nl into one or two blastomeres of two-cell stage *Xenopus* embryos. Rescue experiments were performed with pCS2+MT/XTsh1a linearized with *Not*I and transcribed with SP6 polymerase and pcDNA3/FLmTsh3 linearized with *Not*I and transcribed with T7 polymerase (Manfroid et al., 2004). For lineage tracing, albino embryos were co-injected with 50 pg of LacZ mRNA (Chitnis et al., 1995) or with fluorescein dextran (Molecular Probes), cultivated to the desired stages and stained with X-Gal prior to in situ hybridization.

Whole-mount in situ hybridizations were performed in principle as described (Hollemann et al., 1999). Double staining analysis was carried out according to Hollemann et al. (1998b). Antisense RNA probes were synthesized by in vitro transcription (Stratagene) in the presence of either digoxigenin-rUTP or fluorescein-rUTP (Roche). Synthetic RNA probes were generated using T7 polymerase. The plasmids were cut as follows: Krox-20 with *Eco*RI (Bradley et al., 1993), En-2 with *Xho*I (Hemmati-Brivanlou et al., 1991), Otx-2 with *Not*I (Lamb et al., 1993), Hoxb9 with *Eco*RI (Cho et al., 1988), XPax-6 with *Pst*I (Hollemann et al., 1998a), XTwist with *Xba*I (Hopwood et al., 1989), Hoxa2 with *Not*I (Pasqualetti et al., 2000), Eph-A4 with *Hin*dIII (Smith et al., 1997), Xbap with *Not*I (Newman et al., 1997), AP-2 with *Hin*dIII (Winning et al., 1991), XPAPC with *Xba*I (Kim et al., 1998), Chordin with *Eco*RI (Sasai et al., 1994), Sox2 with *Eco*RI (Mizuseki et al., 1998), Meis3 with *Eco*RI (Salzberg et al., 1999), FGF8 with *Xho*I (Christen and Slack, 1997) and Wnt-4 with *Nhe*I (McGrew et al., 1992).

Vibratome sections

Vibratome sections (30 μm) were prepared as described previously using the Leica VT1000S vibratome (Hollemann et al., 1998b).

Analysis of gene expression using real-time RT-PCR

Total RNA was prepared from embryos using the NucleoSpin® RNA II Kit (Macherey-Nagel). Approximately 150 ng of RNA was used for cDNA synthesis with oligo (dT) primers and MMLV RT (Promega) followed by real-time RT-PCR and quantification using the iCycler® system and iQ SYBR Green Supermix (Bio-Rad) as described by Zhang et al. (2003). Relative expression values were calculated by comparison to a standard curve generated by serial dilution of cDNA. All samples were normalized to levels of *ornithine decarboxylase* (ODC), which was used as a loading control. Samples of water alone or controls lacking reverse transcriptase in the cDNA synthesis reaction failed to give specific products in all cases. Experiments were repeated at least twice on different embryo batches to ensure that the pattern of gene expression described was reproducible from one experiment to the next. Primers for ODC cDNA amplification were the same as designed by Yokota et al. (2003). PCR primer pairs for XTsh1a are listed below:

For: 5′-TGAGTGAGGCGACTGGTTCTACA-3′
Rev: 5′-GCAGCCTGGTGCCAATCATAC-3′

Immunostaining

Single blastomeres of two-cell stage embryos were injected with 400 pg of synthetic MT-XTsh1a mRNA, fixed for 1 h at room temperature in MEMFA (3.7% formaldehyde in 0.1 MOPS, 2 mM EGTA, 1 mM Mg_2SO_4) at gastrula stage and stored at −20°C in 100% ethanol. For histology, the fixed embryos were transferred to 1× APBS (amphibian phosphate-buffered saline, 2.7 mM KCl, 0.15 mM KH_2PO_4, 103 mM NaCl, 0.7 mM Na_2HPO_4, pH 7.5) and embedded in 3% agarose. Transverse sections of 30 μm were cut with a vibratome and collected in concave glass slides for immunostaining. After refixation in MEMFA (10 min, RT), the sections were washed three times with 1× APBS (10 min each) and preincubated in blocking solution (1× APBS, 10% FCS, 1% blocking reagent (BMB, Roche)) for 1 h (4°C). For the primary antibody incubation (anti-myc), the undiluted supernatant of 9E10 hybridomas was applied to the sections for 1 h at 37°C. Following three washing steps (10 min each) in 1× APBS, the sections were treated with secondary antibody (goat-anti-mouse-Cy3, Dianova, diluted in blocking solution) for 1 h at 37°C. Sections were again washed (two times for 10 min in 1× APBS) and treated for 5 min with DAPI solution (0.4 μg/ml in 1× APBS) to visualize the nuclei. To remove excess DAPI, two additional washing steps with 1× APBS were performed. Sections were transferred to a clean glass slide, mounted in elvanol (3 g elvanol and 100 mg phenylene diaminine in 100 ml of a solution containing 30% (v/v) glycerol in 1× APBS) and analyzed on a fluorescence microscope (Leica).

CNC transplantations

Neural crest transplantation assays were essentially performed as described by Borchers et al. (2000). To label the CNC transplants, embryos were injected with either 500 pg of GFP mRNA into one of two blastomeres or 1 ng of dsRED2 mRNA into both blastomeres at the two-cell stage. CNC transplantations were carried out in 1× MBS buffer (10 mM HEPES, pH 7.4, 88 mM NaCl, 1 mM KCl, 2.4 mM Na_2CO_3, 0.82 mM Mg_2SO_4, 0.33 mM Ca $(NO_3)_2$, 0.41 mM $CaCl_2$) at stages 14–15 using only those embryos showing fluorescent labeling in the CNC region. After healing of the grafts (30 min), transplanted embryos were cultivated overnight at room temperature in 0.1× MBS. At stage 26, embryos were examined with a fluorescence stereomicroscope (Leica), and the migration patterns were documented using Open Lab imaging software (Improvision).

Results

Molecular cloning of Teashirt1a and Teashirt1b from Xenopus

Two different cDNA fragments homologous to a partial sequence of mouse Teashirt1 (mTsh1) were amplified from stage 36 cDNA using degenerate primers specific for zinc finger region 2 and 3 of vertebrate Teashirt proteins (Caubit et al., 2000) (Fig. 1A). In successive rounds of RACE, the complete coding sequences of these cDNAs were isolated and termed XTsh1a and XTsh1b. These cDNAs encode proteins of 1078 and 1077 amino acids, respectively, and share nucleotide identities of 94% (94% amino acid identity) and thus likely

represent pseudoalleles (Fig. S1A). XTsh1a and XTsh1b are 78–80% identical to mTsh1 at the amino acid level, but significantly less similar to the two other murine Tsh proteins: mTsh2 and mTsh3 (~46% and ~56% amino acid identity, respectively, Fig. S1B). Resembling their murine and human counterparts (Caubit et al., 2000), both proteins contain three unconventional Tsh type zinc finger motifs (Cx2Cx12HMx4H), a putative homeodomain and two classical zinc finger motifs (Cx2Cx12Hx3-4H) in the C-terminal region (Fig. S1A, Fig. 1A). Because of the indistinguishable expression characteristics of XTsh1a and XTsh1b (not shown), we decided to focus our analysis on XTsh1a.

In *Drosophila*, Tsh protein could be detected both in cytoplasmic and nuclear embryonic fractions, containing hypo- and hyperphosphorylated forms of the protein (Gallet et al., 1999), respectively. XTsh1a contains numerous predicted nuclear localization signals (Fig. S1A). To determine the subcellular distribution of XTsh1a protein *in vivo*, synthetic mRNA encoding an myc-tagged form of XTsh1a was injected into one cell of two-cell stage embryos, which were allowed to develop until mid-gastrula stage (stage 11). The localization of the ectopically expressed protein was traced by immunohistochemistry using a monoclonal antibody recognizing the myc-epitope tags in MT-XTsh1a. Nuclear counterstaining of these sections with DAPI revealed that MT-XTsh1a-specific signals are enriched in the nuclei (Figs. S1C, D). As predicted, XTsh1a therefore appears to function as nuclear protein.

Spatiotemporal expression of XTsh1a during embryogenesis

To determine the temporal expression of XTsh1a, a real-time RT-PCR analysis was performed on RNA preparations from different stages of *Xenopus* embryogenesis. Low levels of transcripts are detected in early blastula stage embryos (Fig. 1B). For better comparison, the amount of transcripts at stage 6 was set to 100%. This maternal XTsh1a RNA decreases during gastrulation. Zygotic transcription is elevated at mid-neurula stages persisting throughout later developmental stages. The spatial expression pattern of XTsh1a was analyzed by whole-mount in situ hybridization on different embryonic stages. Localized XTsh1a expression first becomes evident at early neurula stage in two broad wedge-shaped domains within the neuroectoderm flanking the midline (Figs. 1C, D, F). As neurulation proceeds, these domains are narrowed into bilateral stripes within the neural folds, which converge anteriorly and fuse in the dorsal region of the neural tube (Figs. 1D, E). Throughout neurula stages, the anterior limit of XTsh1a expression is maintained at a position posterior to hindbrain rhombomere 5 (Figs. 1G, H). Similar to mouse Tsh1 (Caubit et al., 2000), neuroectodermal XTsh1a expression is thus early on confined to the trunk region of the prospective CNS, indicating a conservation of these expression characteristics between vertebrates. At stage 26, XTsh1a transcripts are found in a gradient spanning the presumptive hindbrain/spinal cord boundary (Figs. 1I, J), the diencephalon (Fig. 1J), the pronephros (Figs. 1I, J) and the presumptive olfactory placodes (Fig. 1J). Signals within most of these expression domains are

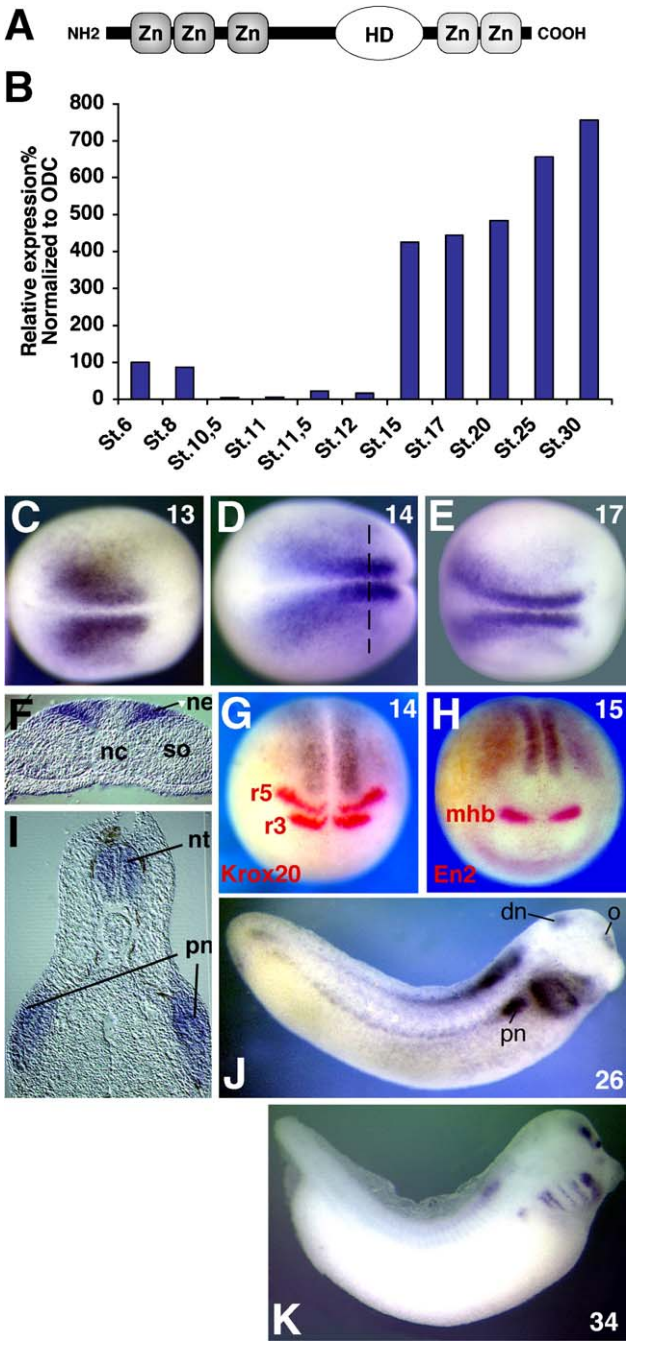

Fig. 1. Structure and expression pattern of XTsh1a. (A) Schematic representation of XTsh1a protein structure. Boxes representing unconventional Teashirt-type Zn finger motifs (Zn) are marked in dark gray, classical Zn finger motifs in light gray, the predicted homeodomain (HD) is indicated in white. (B) Real-time RT-PCR analysis of XTsh1a expression in embryonic stages. Samples were normalized to levels of *ornithine decarboxylase* (ODC). For better comparison, transcript amounts of the stages are shown relative to stage 6 which was set to 100%. (C–E) Spatiotemporal expression of XTsh1a in neurula stages. Dorsal view, anterior is right. (F) Transverse vibratome section corresponding to the dashed line indicated in panel D. (G, H) Double whole-mount in situ hybridization with XTsh1a probe (brown) in combination with Krox-20 (G, red) or En-2 (H, red) probes. Dorsoanterior view, anterior is down. (I–K) Expression of XTsh1a in tailbud embryos. (I) Transverse vibratome section at the hindbrain level (stage 26). (J, K) Lateral view, anterior is right. mhb; midbrain–hindbrain boundary, nc; notochord, ne; neuroectoderm, nt; neural tube, pn; pronephros, r3/r5; rhombomeres 3/5, dn; diencephalon, o; olfactory placode.

still visible at stage 34 but are decreased and spatially retracted (Fig. 1K).

Biphasic expression of XTsh1a in the developing neural crest

From late neurula stage on, expression of XTsh1a becomes detectable in a distinct population of emigrating neural crest cells, which appear to colocalize with Krox-20-positive NC cells of the third branchial arch (Figs. 2A–D). However, sections reveal that XTsh1a expression does not completely overlap with Krox-20 but rather localizes to a medial layer of cells in relation to the more lateral Krox-20-positive cells (Fig. 2F). At stage 26, XTsh1a is expressed in the entire hyoid and branchial arch region (Figs. 1J, 2E). XTsh1a expression is still partially present but strongly reduced in this domain at tailbud stage (Fig. 1K). Thus, XTsh1a is dynamically expressed in two different phases of neural crest migration. First, XTsh1a expression during CNC emigration is found in a restricted population of cells within an individual stream of emigrating branchial CNC cells. Second, XTsh1a is expressed in the posterior postmigratory CNC cells but not in the mandibular subpopulation.

XTsh1a function during anteroposterior neural patterning in Xenopus

Drosophila Tsh acts as a homeotic gene, which is both required and sufficient for the specification of trunk identities during embryogenesis (Fasano et al., 1991; Röder et al., 1992). Ectopic expression of DTsh was reported to induce the homeotic transformation of the labial head segment into the T1 trunk segment of the *Drosophila* embryo (DeZulueta et al., 1994). In heterologous experiments, three murine Tsh orthologues were shown to generate a similar effect in *Drosophila* and to rescue patterning defects in Tsh null mutants (Manfroid et al., 2004). Hence, it appears conceivable that vertebrate Tsh proteins could exert a comparable function in the determination of axial identities in vertebrates.

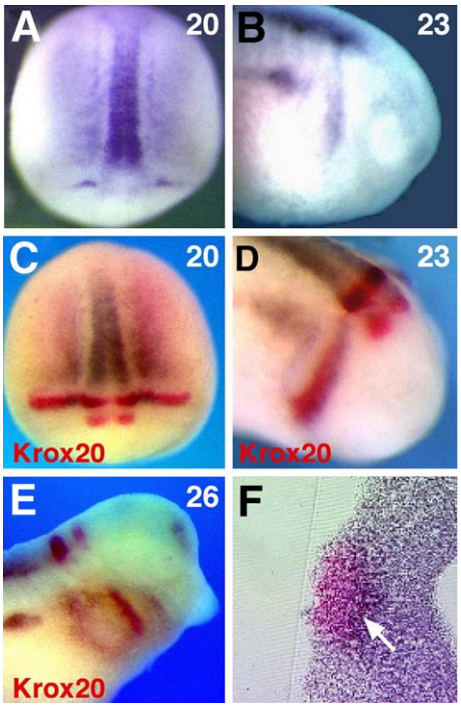

Fig. 2. XTsh1a expression during CNC migration. Whole-mount in situ hybridization of XTsh1a alone (A, B) or XTsh1a (brown) together with Krox-20 (red, C–F). (A, B) Dorsal view, anterior is down. (B, D, E) Lateral view of head region, anterior is right. (F) Horizontal vibratome section of a stage 23 embryo (corresponding to D) stained for Krox-20 (red) and XTsh1a (purple) expression. The white arrow in panel F marks the XTsh1a-positive cell population.

To investigate the function of XTsh1a during AP patterning of the neural plate, we first performed gain-of-function experiments by injecting XTsh1a mRNA into *Xenopus* embryos. Synthetic mRNA encoding full-length XTsh1a was injected into one blastomere of two-cell stage embryos together with mRNA encoding β-galactosidase as lineage tracer. Segment-specific expression of different axial marker genes in *Xenopus* initially arises at mid-neurula stage (stages 14–15), indicating the anteroposterior regionalization of the neural plate. XTsh1a-injected embryos were allowed to develop until stages 14–15 and analyzed for the expression of a panel of AP marker genes (Fig. 3).

Engrailed-2 (En-2), a marker gene for the prospective midbrain/hindbrain boundary (MHB, Hemmati-Brivanlou and Harland, 1989), was found to be reduced or absent in the injected side of XTsh1a-injected embryos (Fig. 3A). Krox-20, a marker gene for rhombomeres 3 and 5 of the hindbrain (Bradley et al., 1993), was also repressed in the manipulated embryos with high frequency (Fig. 3C). XTsh1a-injected embryos were also lacking XPax-6 expression in the hindbrain rhombomeres 3 and 5 (Fig. 3E). However, the more anterior and posterior domains of XPax-6 expression in the eye field and the future spinal cord were still present (Hollemann et al., 1998a). A slight expansion of XPax-6 expression was detected in the prospective eye field, but the domain of XPax-6 in the spinal cord appeared normal (Fig. 3E). Expression of Otx-2, a more anterior marker gene demarcating the region of the prospective forebrain, was also still present in the injected side with a slight reduction of the expression level occurring in a subset of XTsh1a-injected embryos (Fig. 3G, Pannese et al., 1995). The pan-neural marker Sox-2 (Fig. 3I, Mizuseki et al., 1998) and the paraxial and axial mesodermal genes XPAPC (Fig. 3K, Kim et al., 1998) and chordin (data not shown) remained unchanged in their expression when XTsh1a was overexpressed.

To analyze the importance of XTsh1 during embryonic patterning in *Xenopus*, we designed an antisense morpholino oligonucleotide (XTsh1-MO) targeting part of the XTsh1a/b 5′ UTR to knock down XTsh1a/b translation in the embryo. In an *in vitro* translation assay, the XTsh1-MO was capable to inhibit XTsh1a translation (Fig. S2). Interestingly, embryos injected with the XTsh1-MO (referred to as XTsh1 morphants) exhibited AP patterning alterations very similar to those observed in XTsh1a mRNA-injected neurula stage embryos. En-2 and Krox-20 expressions were reduced or repressed completely in XTsh1 morphants (Figs. 3B, D). In addition, XPax-6 expression was repressed in rhombomeres 3 and 5 and expanded anteriorly upon XTsh1-MO injection (Fig. 3F). Comparable to the XTsh1a-injected embryos, Otx-2 expression appeared to be

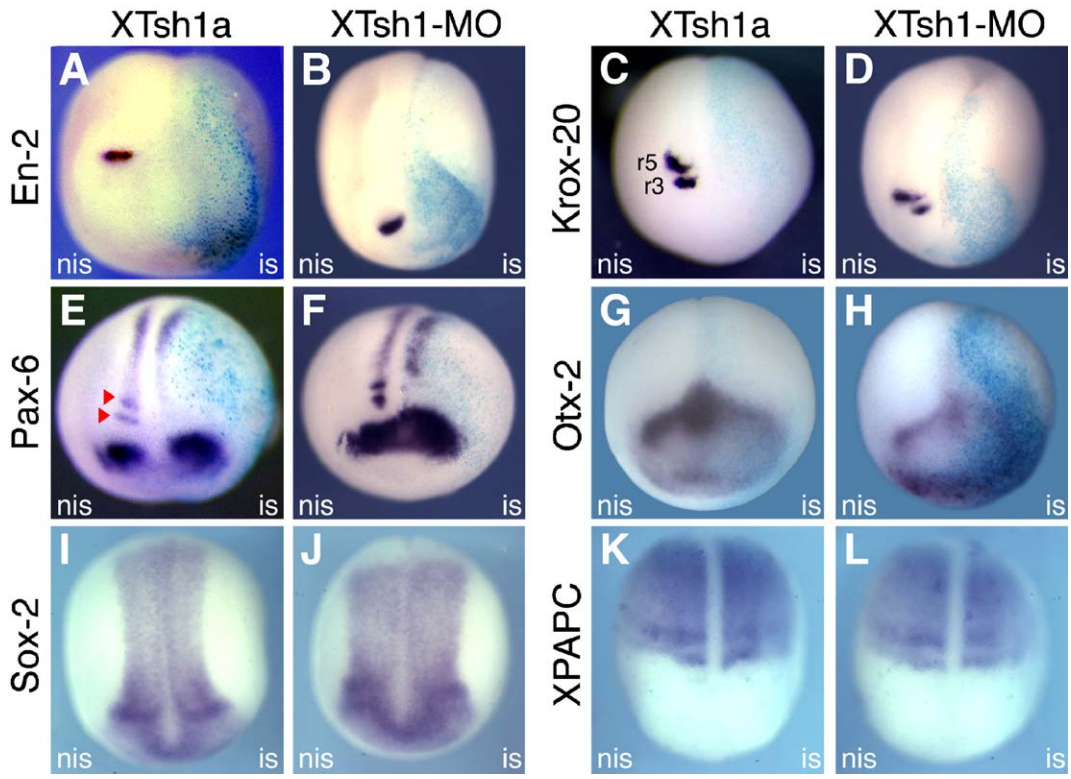

Fig. 3. Anteroposterior neural patterning in XTsh1a-injected embryos and XTsh1 morphants. After injection of XTsh1a mRNA (A, G; 500 pg, C, E; 125 pg) or XTsh1-MO (B, D; 2.5 pmol, F, H; 2 pmol) into one of two blastomeres, embryos were fixed at stages 14–16 and analyzed for the expression of different AP marker genes. Repression or complete loss of En-2 expression (A) appeared in 53% of XTsh1a-injected embryos ($n=26$) and in 36% of XTsh1 morphants ($n=66$). Reduction or absence of Krox-20 expression (B) was detected in 86% of XTsh1a-injected embryos ($n=27$) and in 63% of XTsh1 morphants ($n=119$) (C). XPax-6 expression was found to be reduced in the hindbrain rhombomeres (r3 and r5, red arrowheads) of 57% of the XTsh1a-injected embryos ($n=14$) and in 45% of XTsh1 morphants ($n=104$). (G, H) Otx-2 expression was still detectable in the manipulated side with a slight reduction of the signal intensity occurring in 40% of XTsh1a-injected embryos (G, stage 14, $n=20$) and 50% of XTsh1a morphants (H, stage 14, $n=24$). In XTsh1a mRNA injection experiments, only those embryos were scored, in which the region of marker gene expression overlapped with the staining of the β-galactosidase lineage tracer (light blue). (I, J) Sox-2 (pan-neural marker) expression remains unchanged. (K, L) XPAPC (paraxial mesoderm marker) expression was not altered. In panels I–L, fluorescein dextran was used as lineage tracer. is: injected side, nis: non-injected side. Anterior pole of the embryos is orientated to the lower edge of the frame.

faintly reduced in the injected side of XTsh1 morphants (Fig. 3H). Importantly, the pan-neural marker Sox2 (Fig. 3J) and the mesodermal markers XPAPC (Fig. 3L) and chordin (data not shown) remained unchanged. When the control morpholino was injected, marker gene expression remained unaffected (data not shown).

To further confirm the specificity of the XTsh1 morphant phenotype, rescue experiments were performed with XTsh1a-ORF lacking the antisense morpholino binding site (Fig. S2) and with murine teashirt (mTsh3, Fig. S1). Both injected RNAs rescued Krox-20 expression in a dose-dependent manner with optimal concentrations of 50 pg for mTsh3 and 25 pg for XTsh1 (Table 1, Fig. S3).

Since XTsh1 is not expressed in the hindbrain, but was found to influence spatially restricted hindbrain genes, we investigated its effect on Wnt-4 and Meis3 expression. Both overlap with the teashirt expression domain in the trunk region (McGrew et al., 1992; Salzberg et al., 1999), and Meis3 has been reported to control hindbrain patterning (Salzberg et al., 1999; Aamar and Frank, 2004). Ectopic expression of XTsh1a had no effect on both genes (Figs. 4A, E). In the XTsh1 morphant, however, Wnt-4 expression was reduced in brain and spinal cord (Fig. 4B). Meis3 expression shifted posteriorly, which became more clear during neural tube closure at stage 19 (Figs. 4F, G). Expression of FGF-8, as a further signal molecule important for AP patterning of the neural ectoderm (Kudoh et al., 2002), remained unchanged (Figs. 4C, D). Rescue experiments with optimal concentrations of XTsh1a-ORF and mTsh3 led to recovery of Meis3 and Wnt-4 expression (Table 1, Fig. S3) and further confirmed the specificity of the XTsh1-MO phenotype.

Effects of XTsh1a on neural crest development

Because of the differentially regulated expression of XTsh1a in neural crest structures, we were interested to determine if neural crest development was also affected by ectopic expression of XTsh1a. To identify NC cells, XTsh1a-injected neurula stage embryos were monitored for the expression of Twist, an early NC marker gene (Hopwood et al., 1989). Twist expression in NC progenitors at the lateral margins of the neural plate appeared normal in XTsh1a-injected neurula stage embryos, indicating that NC induction could proceed properly in these embryos (Fig. 5A). However, in later stages, the segmental array of hyoid and branchial CNC streams expressing

Table 1
Rescue of Krox-20, Wnt-4 and Meis3 expression in *Xenopus* embryos co-injected with XTsh1-MO and XTsh1a or mTsh3 mRNA

Co-injection of 2.5 pmol XTsh1-MO and different concentrations of XTsh1a or mTsh3 mRNA	Experimental embryos	Krox-20 phenotype[a]	Wild-type embryos	Number of experiments
Control	83	63 (76%)	20 (24%)	7
XTsh1a (10 pg)	36	28 (78%)	8 (22%)	2
XTsh1a (25 pg)	93	40 (43%)	53 (57%)	7
XTsh1a (50 pg)	28	15 (54%)	13 (46%)	3
XTsh1a (250 pg)	28	19 (68%)	9 (32%)	2
mTsh3 (10 pg)	55	18 (33%)	37 (67%)	4
mTsh3 (25 pg)	47	13 (28%)	34 (72%)	4
mTsh3 (50 pg)	21	18 (86%)	3 (14%)	1
	Experimental embryos	XWnt-4 phenotype[a]	Wild-type embryos	Number of experiments
Control	66	45 (68%)	21 (32%)	5
XTsh1a (25 pg)	41	18 (44%)	23 (56%)	3
mTsh3 (50 pg)	38	17 (45%)	21 (55%)	3
	Experimental embryos	XMeis3 phenotype[a]	Wild-type embryos	Number of experiments
Control	54	41 (76%)	13 (24%)	5
XTsh1a (25 pg)	39	16 (41%)	23 (59%)	3
mTsh3 (50 pg)	40	19 (48%)	21 (52%)	3

Xenopus embryos were unilaterally co-injected with 2.5 pmol XTsh-MO and different concentrations of XTsh1a or mTsh3 RNA as listed above. Krox-20, XWnt-4 and XMeis3 expression in the non-injected side was compared with the unilaterally co-injected side of the same embryo.

[a] Reduced expression or loss of the Krox-20 and XWnt-4 signal and posteriorly shifted XMeis3 expression was defined as phenotype. Optimal rescue conditions were obtained for 25 pg XTsh1a RNA or 50 pg mTsh3 RNA injections. Control: only XTsh1-MO was injected.

Twist was severely disrupted in the injected side (Figs. 5B, C). CNC cells were still present at the hyoid and branchial arch level in XTsh1a-injected embryo; however, they did not migrate ventrally as separate streams but were rather clustered and retained in a dorsal position (Figs. 5B, C). The expression pattern of the NC marker gene AP-2 (Winning et al., 1991) also appeared severely disorganized in XTsh1a-injected embryos (Figs. 5E, F). Because the failure of CNC cells to colonize the pharyngeal arches in XTsh1a-injected embryos could result from defects in the pharyngeal morphology, we analyzed this region in horizontal sections. In the manipulated side of the embryos, segmentation of the pharyngeal pouches appeared abnormal, exhibiting fused segments (Fig. 5D). Therefore, the CNC malformations in XTsh1a-injected embryos might partly ensue from the irregular development of the pharyngeal arches, the CNC target structures.

In XTsh1 morphants, extensive CNC patterning defects could only be observed at neurula stage. Neural crest induction was not affected in XTsh1-MO-injected embryos (Fig. 5G). However, at late neurula stages, it became obvious that Twist-expressing CNC segments did not separate properly in a subset of XTsh1 morphants (Fig. 5G). At later stages, Twist expression in the branchial arches only appeared mildly reduced and disorganized (Figs. 5H–J).

Thus, the formation of CNC segments also appears to be disturbed by positively and negatively interfering with XTsh1 levels in the embryo, suggesting an important function for XTsh1 in the segmental organization of the CNC.

Misexpression of XTsh1a interferes with the acquisition of posterior CNC identities

To further characterize the CNC migration defects, we investigated if marker genes indicative for specific crest streams were still expressed in the manipulated embryos. The restricted expression of ephrin signaling receptors and ligands in specific NCC streams is critical for the segregation of the CNC into well-defined migrating streams in *Xenopus* (Smith et al., 1997). EphA4 is expressed in migrating NCC destined for the third

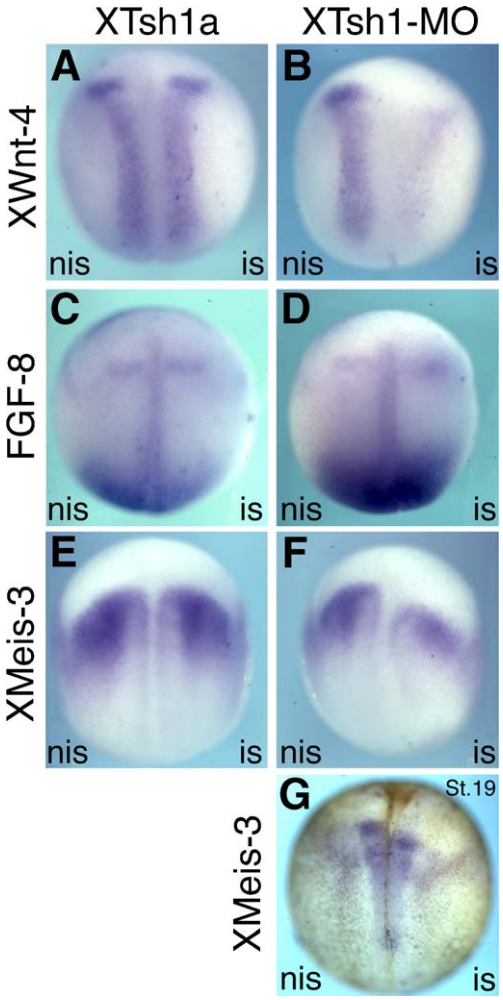

Fig. 4. Analysis of genes regulating brain patterning in XTsh1a-injected embryos and XTsh1 morphants. (A, B) XWnt-4 expression is unchanged in XTsh1a-injected embryos but repressed in XTsh1 morphants. (C, D) FGF-8 expression remains unaffected. (E–G) XMeis3 expression is unchanged in XTsh1a-injected embryos but shifts posteriorly in XTsh1 morphants. A–F: albino embryos of stage 16 were used for in situ hybridization, G: wild-type embryo of stage 19 is shown. Embryos were injected with XTsh1a mRNA (500 pg) or XTsh1-MO (2.5 pmol) into one of two cells. Fluorescein dextran was used as lineage tracer. is: injected side, nis: non-injected side. Anterior pole of the embryos is orientated to the upper edge of the frame.

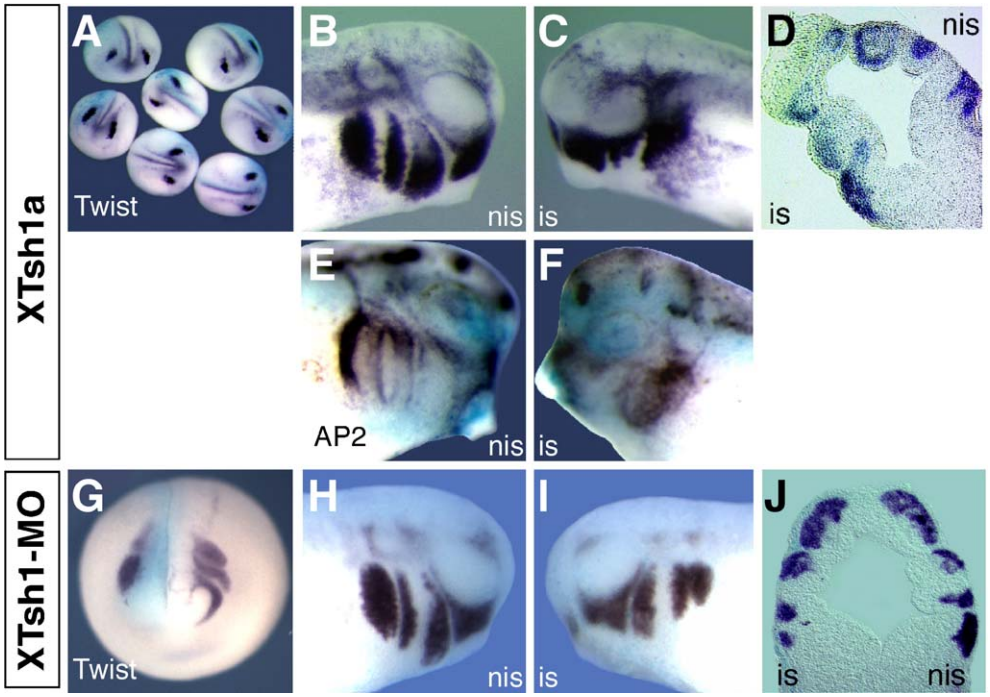

Fig. 5. CNC development in XTsh1a-injected embryos and XTsh1 morphants. Embryos were injected with XTsh1a mRNA (500 pg) or XTsh1-MO (2.5 pmol) into one of two cells, fixed at stage 16 (A), 19 (G) or 26 (B–F, H–J) and stained for the expression of the NC marker genes Twist (A–D, G–J) and AP-2 (E, F). At neurula stage, Twist expression was not altered in 88% ($n=17$) of XTsh1a-injected embryos (A). Although manipulated embryos still express Twist at tailbud stage (stage 26), the expression pattern appears severely disorganized in the hyoid and branchial arches in 68% (C, $n=62$) of the XTsh1a-injected embryos. Disruption of AP-2 expression occurred with similar frequencies (E, F). In XTsh1 morphants, Twist expression was also not reduced at late neurula stage (G). However, segmental patterning of the CNC streams appeared abnormal in 52% ($n=25$) of the XTsh1-MO-injected embryos (G). At tailbud stage (H, I, stage 26), Twist was reduced in 48% and detected in a slightly irregular shape in 31% of XTsh1 morphants ($n=29$). (D, J) Horizontal vibratome sections of the branchial arch region of Twist-stained embryos (stage 26) injected with XTsh1a (D, 500 pg) or XTsh1-MO (J, 2.5 pmol). Defective segmentation of the pharyngeal pouches is revealed in the injected side of XTsh1a-injected embryos (D) but not evident in XTsh1-MO-injected embryos at this stage (J), which exhibit reduced numbers of Twist-expressing cells in the CNC streams. is: injected side, nis: non-injected side.

arch, in third arch mesoderm and in rhombomeres 3 and 5 of the hindbrain (Winning and Sargent, 1994; Xu et al., 1995). Ectopic expression of a truncated form of the EphA4 receptor blocking its signaling function leads to the aberrant migration of third arch NCC into territories of the second and fourth arch (Smith et al., 1997). EphA4 expression in CNC cells and r3/r5 was strongly reduced or eliminated in manipulated embryos (Figs. 6E, F). In parallel, Krox-20 expression in the third arch and hindbrain was as well absent or severely repressed upon ectopic expression of XTsh1a (Figs. 6A, B). Hoxa2, a marker gene of second arch CNC, acts as selector of hyoid identity in vertebrates (Pasqualetti et al., 2000; Rijli et al., 1993). XTsh1a-injected embryos almost completely lacked Hoxa2 expression in the CNC and the hindbrain (Figs. 6I, J). However, Xbap (Newman et al., 1997) was still expressed at its proper site in the mandibular CNC of XTsh1a-injected embryos but reduced in the hyoid and branchial CNC (Figs. 6K, L).

XTsh1-MO injection had only weak effects on the establishment of anteroposterior CNC identities at tailbud stages. A reduction of Krox-20 and EphA4 expression in the third CNC stream was observed in few XTsh1 morphants (Figs. 6C, D, G, H), possibly reflecting transient effectiveness of the XTsh-MO.

Taken together, these observations suggest that ectopic XTsh1a inhibits the acquisition of CNC identities in the second and more posterior arches, but not the specification of first arch CNC. The CNC migration defects in XTsh1a-injected embryos could therefore also arise from the loss of posterior CNC identities, possibly impeding regional CNC pathfinding.

Neural crest migration defects in XTsh1a-injected embryos specifically affect posterior CNC pathways

Since the observations made to this point did not allow us to distinguish if the migration defects in CNC of XTsh1a-injected embryos were based on cell-intrinsic or -extrinsic mechanisms, we made use of an NC transplantation assay (Borchers et al., 2000). Fluorescence-labeled explants were taken from the CNC region of neurula stage embryos that had been unilaterally injected with GFP mRNA either alone or together with XTsh1a mRNA or XTsh1-MO (Fig. 7). These explants were grafted into the corresponding region of non-injected host embryos, from which an explant of equal size had previously been removed. The embryos were cultivated until stage 26 at which the migration patterns of the GFP-labeled CNC streams were documented and scored. Depending on the axial position of the graft in the host embryo, transplanted GFP-labeled CNC cells entered either the mandibular NC streams (Figs. 7A, B) from anterior

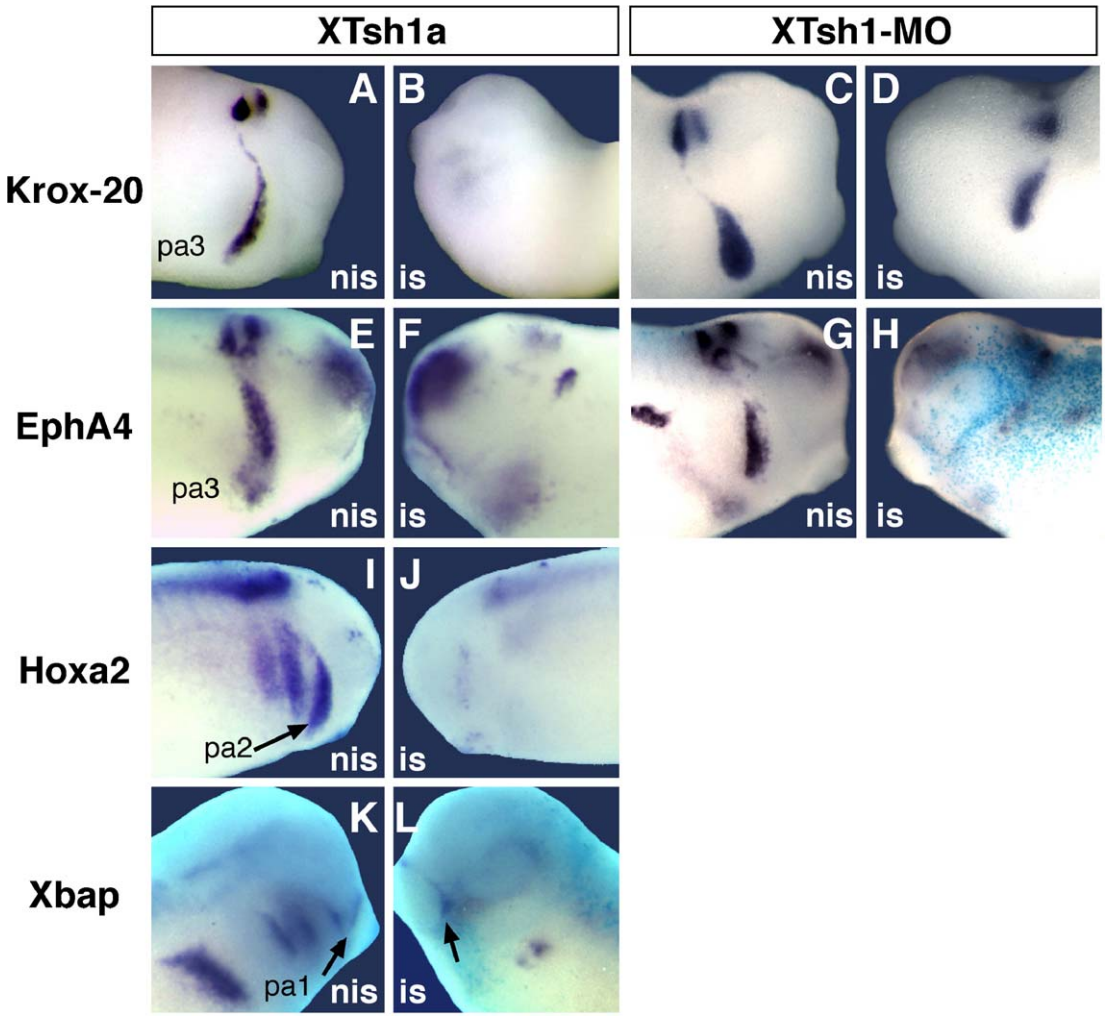

Fig. 6. Analysis of segmental CNC identities in *Xenopus* embryos upon overexpression and knockdown of XTsh1. Following injection of XTsh1a mRNA (A, B, E, F, I–L; 500 pg) or XTsh1-MO (C, D; 2.5 pmol, G, H; 2 pmol) into one of two blastomeres, embryos were fixed at stage 26 and analyzed for the expression of marker genes for the different pharyngeal arch segments. XTsh1-injected embryos exhibit strongly or completely reduced expression of the third arch marker genes Krox-20 (A, B, 84%; $n=19$) and EphA4 (C, D, 60%; $n=20$). Similar effects were observed in XTsh1a morphants, where CNC domains of Krox-20 (C, D) and EphA4 (G, H) were reduced in 56% ($n=18$) and 8% ($n=26$), respectively. XTsh1a-injected embryos also revealed a reduced expression of the second arch marker gene Hoxa2 (arrow, I, J, 55%, $n=20$). Although reduced Xbap expression was observed in posterior pharyngeal arches of the XTsh1a-injected embryos (25%; $n=20$), Xbap expression in the first pharyngeal arch (arrowheads in K and L) was not affected. is: injected side, nis: non-injected side, pa; pharyngeal arch.

positions or the hyoid and branchial CNC streams from more posterior levels (Figs. 7E, F). Co-injection of the XTsh1-MO did not affect CNC migration in this assay (Figs. 7I, J, Table 2).

When XTsh1a was coexpressed in CNC explants, however, only the mandibular CNC cells followed a normal migration route in the majority of embryos (Figs. 7C, D, Table 2). XTsh1a-expressing CNC grafts did not colonize the posterior arches in distinct streams, but remained in a more dorsal position with a high frequency (Figs. 7G, H, Table 2). In time-lapse analyses, we could observe that XTsh1a-expressing CNC cells initially started to migrate, but they did not segregate in the pharyngeal region (not shown). Therefore, posterior XTsh1a-misexpressing CNC cells are apparently capable to migrate but unable to follow their appropriate migration pathways, suggesting that CNC migration defects in XTsh1a-injected embryos are based on a cell-autonomous mechanism.

However, the segmentation defects of posterior pharyngeal arches implied that the tissue environment providing external cues for CNC migration was also altered in XTsh1a-injected embryos. Thus, we characterized the migration behavior of GFP-labeled control CNC grafts in XTsh1a-injected embryos co-injected with dsRED2 or βGal mRNA as a lineage tracer. GFP-labeled control CNC did not form segregated streams in XTsh1a-injected embryos, and CNC migration was also retarded in a subset of these embryos (Fig. 7K, Table 2). Therefore, the CNC migration defects observed upon XTsh1a misexpression appear to rely on a combination of changes in the cell-autonomous properties of CNC cells and the non-cell-autonomous properties of CNC migration environment.

Because the migration defects in XTsh1a-expressing CNC grafts appeared to specifically affect posterior CNC populations, we were interested to analyze if these grafts would still

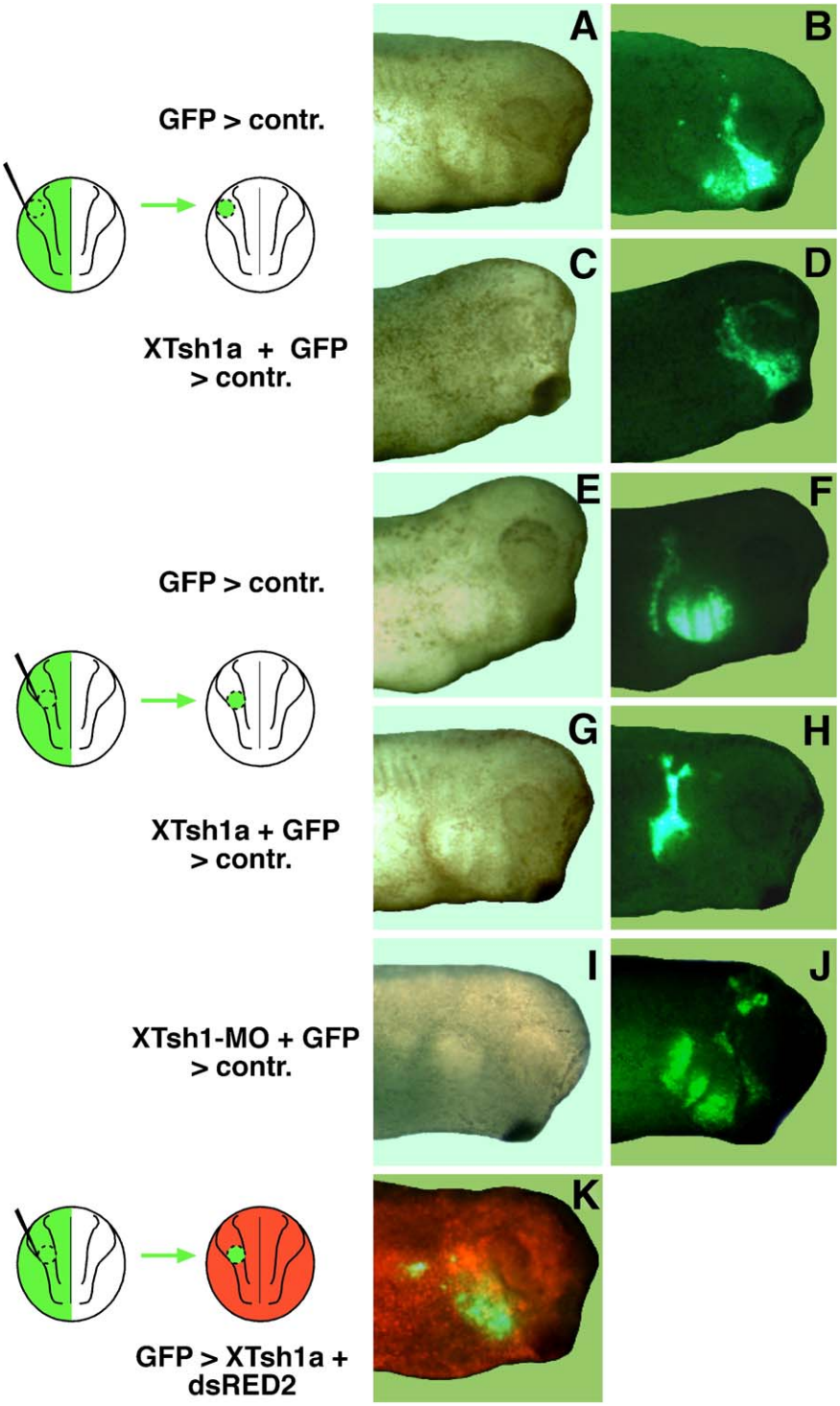

Fig. 7. XTsh1 misexpression inhibits branchial CNC migration. GFP-labeled CNC grafts were taken from anterior (A–D) or posterior (E–J) levels of control embryos (A, B, E, F), XTsh1a-injected embryos (500 pg, C, D, G, H) or XTsh1 morphants (2.5 pmol, I, J) and transplanted to uninjected host embryos. (K) Transplantation of a GFP-labeled control CNC graft to the posterior region of a host embryo, which had been co-injected with XTsh1a (1 ng) and dsRED2 (1 ng) mRNA into both blastomeres of the two-cell stage. Transplantations were performed at neurula stage (stage 14), and migration patterns were evaluated at stage 26. Normal light images and corresponding fluorescent images of the head region of representative examples are shown (anterior is right).

be able to follow normal migratory routes when transplanted to heterotopic anterior positions. To internally control the positioning of grafts, we simultaneously transplanted GFP-labeled control CNC and dsRED2-labeled XTsh1a-expressing CNC into either anterior or posterior levels of non-injected host embryos (Fig. 8). In both homo- and heterotopic transplantations, XTsh1a-expressing CNC cells were able to colonize the region of the mandibular arch, but not the more posterior arches (Figs. 8A–D). Regardless of their axial level of origin, CNC cells ectopically expressing XTsh1a therefore

Table 2
Influence of XTsh1a on CNC migration at different axial levels

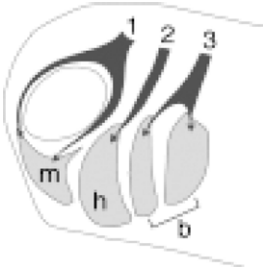

Type of transplantation # of embryos	Pharyngeal arch	CNC migration	
		+	Retarded
GFP>control $n=18$	Mandibular (1)	10	
	Hyoid (2)	14	
	Branchial (3)	8	1
GFP+XTsh1a>control $n=27$	Mandibular (1)	11	3
	Hyoid (2)	3	1
	Branchial (3)		12
GFP+XTsh1-MO>control $n=16$	Mandibular (1)	4	
	Hyoid (2)	11	
	Branchial (3)	13	2
GFP>XTsh1a+dsRED2/βGal $n=34$	Not specified	22	12

GFP-labeled migration patterns in CNC-transplanted embryos were scored separately at different axial levels. Migration patterns of mandibular (m), hyoid (h) and branchial (b) pathways were classified either as normal (+) or retarded (see examples in Figs. 7 and 8). A complete inhibition of CNC migration was not observed in any case. Segmental CNC migration pathways could not well be discriminated in XTsh1a-injected recipient embryos and were thus not distinguished in the evaluation (bottom row). Here, we also integrated the results of experiments in which the recipient embryos were co-injected with β-galactosidase mRNA and processed for X-Gal staining, alternatively. In our analysis, we only considered those embryos in which the signals of the lineage tracer (dsRED2, βGal) were surrounding the GFP-labeled transplants.

remain competent to sense and follow the mandibular CNC migration pathway, confirming the specificity of the effect. Our results therefore provide evidence for differential requirements in migratory competence for the XTsh1a-insensitive mandibular pathway and for the XTsh1a-sensitive posterior pathways.

Discussion

Here, we describe the identification and characterization of two pseudoallelic homologues of Tsh1 from *Xenopus*, XTsh1a and XTsh1b (collectively referred to as XTsh1), with equal expression characteristics in segmentally restricted domains of the developing brain and CNC. To determine the function of XTsh1 during embryonic patterning, we performed gain- and loss-of-function experiments by ectopically expressing XTsh1a or injecting XTsh1 antisense MO oligonucleotides, respectively. Overexpression and depletion of XTsh1 were found to affect two major processes of neural regionalization: primary AP patterning of the CNS and segmentation of the CNC. Moreover, segmental specification was abolished in posterior CNC upon XTsh1a overexpression.

Influence of XTsh1a on posterior brain specification

Similar to the expression characteristics of the murine Tsh1 and Tsh2 in the embryonic trunk region (Caubit et al., 2000), we find that XTsh1 expression is confined to the posterior region of the prospective CNS during early neurula stages with the anterior limit mapping to a position caudal to rhombomere 5 (Figs. 1, 2). XTsh expression is initiated at neurula stage and thus follows the establishment of nested Hox gene expression, which already takes place at gastrula stage in *Xenopus* (Wacker et al., 2004). Similar to *Drosophila* tsh, XTsh1 expression thus could be controlled by homeotic genes (McCormick et al., 1995). Ectopic expression of XTsh1a at other levels of the neuraxis strongly interferes with the acquisition of MHB and hindbrain identities. Our data thus demonstrate that, in addition to the AP patterning activities of murine Tsh genes in *Drosophila* (Manfroid et al., 2004), vertebrate segmental patterning is also sensitive to alterations in Tsh1 levels. However, apart from the anterior expansion of XPax-6, we could not identify markers that are upregulated or shifted in response to ectopic XTsh1a. Therefore, we could not detect homeotic transformations of axial identities reminiscent of those reported in *Drosophila*. The almost complete and selective absence of prospective mid- and hindbrain markers in XTsh1-depleted and XTsh1a mRNA-injected embryos is striking.

Since the anterior limit of XTsh1a expression is restricted to a level posterior to the prospective hindbrain region, the observed effects could be mediated indirectly by downstream factors of XTsh1 acting at long range, which are important for the determination of mid/hindbrain fates. Strong experimental evidence is provided by the observation that Wnt-4 is downregulated and XMeis3 expression shifted posteriorly upon knockdown of XTsh1. XMeis3 is part of transcriptional activator complexes and able to induce En-2 and Krox-20 in the absence of pan-neural genes (Dibner et al., 2001). XMeis3 activates the FGF/MAPK signaling pathway in non-cell-autonomous manner which leads to a caudalization of neural tissue (Aamar and Frank, 2004). Wnt/β-catenin signaling also plays an important role in posteriorization of the neural tissue (Kiecker and Niehrs, 2001; Kudoh et al., 2002). Functional studies specific for XWnt-4 in brain patterning have not been reported to date. Overexpression of Tsh1a did not alter XWnt-4 or Meis3 expression so that the loss of hindbrain markers like en and Krox-20 remains unexplained in the gain-of-function situation. Therefore, we assume that additional unknown effectors might be involved in mediating the teashirt function. Apart from that, the loss-of-function analysis underlines that XTsh1 affects the expression of genes that possess the capacity for long-distance regulation.

In *Drosophila*, tsh has been reported to cooperate with the homeotic gene *Scr* in the definition of the first trunk segment (T1) in the *Drosophila* embryo (Röder et al., 1992; DeZulueta et al., 1994). Furthermore, an interaction between teashirt and homothorax, the *Drosophila* Meis homologue, was demonstrated by Bessa et al. (2002). Given the

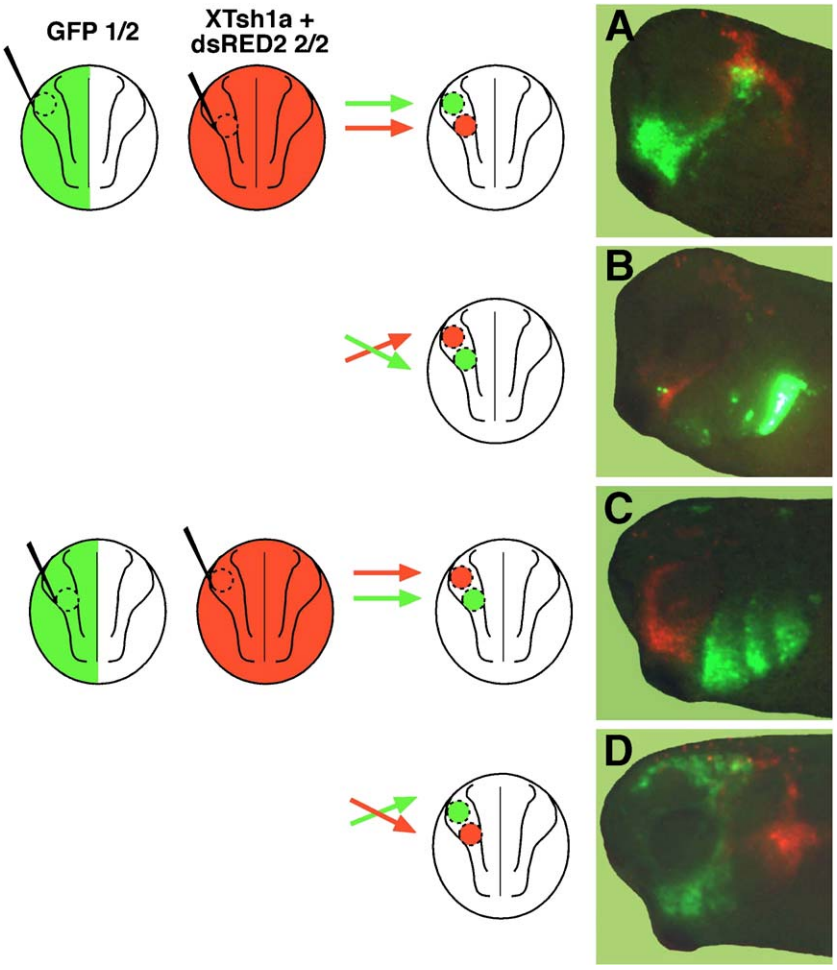

Fig. 8. Selective influence of XTsh1a on posterior CNC migration pathways. For double transplantation experiments, control CNC grafts were labeled with GFP (500 pg, 1/2 cells) and XTsh1a-expressing grafts (1 ng, 2/2 cells) were labeled with dsRED2 (1 ng, 2/2 cells). The grafts were either placed to the axial position corresponding to their origin (homotopic; A, C) or interchanged to more posterior or anterior positions (heterotopic; B, D) of uninjected host embryos. Merged fluorescent images show typical results.

evolutionary conservation of Tsh protein activities, which we confirmed with our mTsh3 rescue experiments, it seems conceivable that XTsh1 might also act in concert with Hox genes.

The nuclear localization of XTsh1a protein detected here is compatible with its function in transcriptional repression already known for DTsh and murine Tsh homologues (Manfroid et al., 2004; Waltzer et al., 2001). Evidence from *Drosophila* suggested that Tsh might function as a component of a ternary repressor complex regulating *Ubx* expression in the midgut (Saller et al., 2002). Thus, the observed effects might not rely on a direct role of XTsh1a in transcriptional regulation, but on their interference with the formation of an XTsh1-containing regulatory complex. This could also provide an explanation for the similarity of effects obtained by negative and positive alterations in XTsh1 levels. In different manners, both manipulations might disrupt the formation of a transcription complex; in the knockdown situation due to a lack of XTsh1 protein and in the overexpression situation as a result of imbalanced complex stoichiometry caused by excessive XTsh1 protein.

Selective effect of XTsh1a on segmental identities and migratory routes of posterior CNC

Comparable to our results showing late expression of XTsh1a in postmigratory CNC (Figs. 1, 2), murine Tsh1 was reported to be expressed in the distal domains of branchial arches 1 and 2 at 11 d.p.c. (Caubit et al., 2000). However, in *Xenopus*, the expression of XTsh1 is more prominent as the hyoid and branchial arches are completely positive for XTsh1 at postmigratory stages. Furthermore, we observed an early expression of XTsh1 in a subpopulation of migratory CNC cells of the third arch, which appears not to be evident in mice. Since murine Tsh genes are able to replace the *Drosophila* homologue in defining trunk identity (Manfroid et al., 2004), the question arises what is the function of these genes in the cranial neural crest, a tissue which is not found in invertebrates.

Similar to the results of XTsh1a overexpression, we find that XTsh1-MO injection affected CNC segmentation; however, the more obvious effects were detected in early stages of CNC development. The reduced occurrence of XTsh1-MO effects in later stages of CNC development and the lack of XTsh1-MO

effects in CNC transplantation assays might owe to the temporally limited activity of the morpholino. Alternatively, the morpholino may cause a delay in CNC migration resulting in a weaker phenotype. Nevertheless, the similar effects on CNC segmentation obtained by injection of XTsh1 mRNA and XTsh-MO indicate an important function of XTsh1 in this process, which might be linked to its earlier role in neural regionalization.

XTsh1a misexpression interferes with the proper migration and segmental specification of posterior CNC streams, but not the most anterior (mandibular) CNC stream (Fig. 6). Premigratory CNC transplanted from one axial level of the CNS to another follows the migration pathways appropriate for their new position. Thus, CNC cells initially appear to be plastic in their competence to perceive the environmental cues guiding them to different destinations along the AP axis. This has already been observed by Hörstadius and Sellman (1946). In XTsh1a-injected embryos, this plasticity appears to be disturbed with regard to their ability to follow posterior, but not mandibular routes (Fig. 8). In this aspect, XTsh1 seems to control posterior but not anterior identity of the CNC subpopulation but as in the brain it is not able to induce anterior to posterior (mandibular to branchial) transformations. Since XTsh1a is expressed in a medial subset of migrating third arch CNC cells, it may delimit CNC migration of the more superficial Krox-20-positive CNC cells. The selective effect of XTsh1a on migratory competence of posterior CNC, but not the mandibular crest, is reminiscent of observations reported by Alfandari et al. (2001). In this study, it was demonstrated that *Xenopus* CNC cell grafts that express protease-defective ADAM 13 fail to migrate along the hyoid and branchial pathway, but migrate normally along the mandibular pathway. In combination with this study, our data might therefore reflect general differences in the requirements of CNC migration along anterior vs. posterior pathways. The absence of Hox gene expression in the most anterior segment of the CNC (Hunt et al., 1991) may account for these differences. Although both XTsh-injected and defective ADAM 13 CNC grafts only affect the posterior CNC, they differ extremely in the migratory phenotype. Grafted XTsh1a-overexpressing CNC start migration but half on their way they stop and are unable to find their routes to the different visceral arches (Figs. 7 and 8). In contrast, most of the defective ADAM-13-expressing CNC do not start migration, some chose the mandibular instead of the branchial route (Alfandari et al., 2001). Expression of the truncated Eph receptors also shows a different phenotype as CNC migrate but failed to separate properly into the different visceral arches (Smith et al., 1997; Helbling et al., 1998).

Our converse transplantations further demonstrate that XTsh1 not only affects the migratory behavior of the CNC (intrinsic effect). It also alters the cellular environment so that wild-type CNC are unable to enter the visceral arches (extrinsic effect) (Fig. 7I and Table 1). The extrinsic effect appeared less severe (55% retardation) than the intrinsic one (87% retardation). The extrinsic effect might be due to failures in segmentation of the pharyngeal pouches (Fig. 5D), which could result in disorientation of the migrating CNC. Interestingly, Hörstadius and Sellman (1946) observed in their extirpation and grafting experiments that the pharynx–endoderm influences the migration and differentiation of the CNC. Excision of the pharynx wall led to complete lack of cartilaginous arches. In addition, they demonstrated that CNC transplanted into the trunk region only differentiated to cartilaginous structures when pharynx–endoderm was added to the graft. Remarkably, in these combined grafts, cartilage and secondary gill slits were formed. From their and our data, it seems tempting to speculate that the migratory competence of posterior CNC and also the segmentation of the pharynx wall depend on Hox proteins. As discussed earlier, *Drosophila* Tsh was shown to collaborate with certain Hox genes like *Scr*, *HOM-C*, *Hth*, *ANTP-C* and *BX-C* (DeZulueta et al., 1994; Alexandre et al., 1996; Bessa et al., 2002; Röder et al., 1992). But it has also been reported that DTsh in complex with brinker and CtBP represses *Ubx* (Waltzer et al., 2001; Saller et al., 2002). If AP patterning of the CNC and the pharynx wall involves Hox gene activity, it seems most likely that XTsh1 overexpression alters the competence of both tissues to respond to positional signals. Indeed, Hox genes have been shown to be involved in the regionalization of the vertebrate gut (Roberts et al., 1998; Sekimoto et al., 1998). We found Hoxa2 suppressed by XTsh1 in the hyoid and branchial arches (Fig. 6). Further investigations are necessary to confirm whether analogous regulatory mechanisms pattern the pharyngeal region.

Acknowledgments

The authors would like to thank David Wilkinson, Paul Krieg, Filippo Rijli, Frank Dale and Laurent Fasano for providing plasmids. We further thank Christine Van Lishout, Marco Winkler and Ines Eckhardt for technical assistance. This work was funded by grants from the DFG to D.W. and T.P. and by a grant from the Helmholtz-Gemeinschaft to D.W.

Appendix A. Supplementary data

Supplementary data associated with this article can be found, in the online version, at doi:10.1016/j.ydbio.2006.06.041.

References

Aamar, E., Frank, D., 2004. *Xenopus* Meis3 protein forms a hindbrain-inducing center by activating FGF/MAP kinase and PCP pathways. Development 131, 153–163.

Alexandre, E., Graba, Y., Fasano, L., Gallet, A., Perrin, L., de Zulueta, P., Pradel, J., Kerridge, S., Jacq, B., 1996. The *Drosophila* teashirt homeotic protein is a DNA-binding protein and modulo, a HOM-C regulated modifier of variegation, is a likely candidate for being a direct target gene. Mech. Dev. 59, 191–204.

Alfandari, D., Cousin, H., Gaultier, A., Smith, K., White, J.M., Darribère, T., DeSimone, D.W., 2001. *Xenopus* ADAM 13 is a metalloprotease required for cranial neural crest migration. Curr. Biol. 11, 918–930.

Bessa, J., Gebelein, B., Pichaud, F., Casares, F., Mann, R.S., 2002. Combinatorial control of *Drosophila* eye development by eyeless, homothorax, and teashirt. Genes Dev. 16, 2415–2427.

Borchers, A., Epperlein, H., Wedlich, D., 2000. An assay system to study

migratory behaviour of neural crest cells in *Xenopus*. Dev. Genes Evol. 210, 217–222.

Borchers, A., David, R., Wedlich, D., 2001. *Xenopus* cadherin-11 restrains cranial neural crest migration and influences neural crest specification. Development 128, 3049–3060.

Bradley, L.C., Snape, A., Bhatt, S., Wilkinson, D.G., 1993. The structure and expression of the *Xenopus* Krox-20 gene: conserved and divergent patterns of expression in rhombomeres and neural crest. Mech. Dev. 40, 73–84.

Caubit, X., Core, N., Boned, A., Kerridge, S., Djabali, M., Fasano, L., 2000. Vertebrate orthologues of the *Drosophila* region-specific patterning gene teashirt. Mech. Dev. 91, 445–448.

Chitnis, A., Henrique, D., Lewis, J., Ish-Horowicz, D., Kintner, C., 1995. Primary neurogenesis in *Xenopus* embryos regulated by a homologue of the *Drosophila* neurogenic gene Delta. Nature 375, 761–766.

Cho, K.W., Goetz, J., Wright, C.V., Fritz, A., Hardwicke, J., De Robertis, E.M., 1988. Differential utilization of the same reading frame in a *Xenopus* homeobox gene encodes two related proteins sharing the same DNA-binding specificity. EMBO J. 7, 2139–2149.

Christen, B., Slack, J.M., 1997. FGF-8 is associated with anteroposterior patterning and limb regeneration in *Xenopus*. Dev. Biol. 192, 455–466.

deZulueta, P., Alexandre, E., Jacq, B., Kerridge, S., 1994. Homeotic complex and teashirt genes co-operate to establish trunk segmental identities in *Drosophila*. Development 120, 2287–2296.

Dibner, C., Elias, S., Frank, D., 2001. XMeis3 activity is required for proper hinbrain patterning in *Xenopus laevis* embryos. Development 128, 3415–3426.

Eickholt, B.J., Mackenzie, S.L., Graham, A., Walsh, F.S., Doherty, P., 1999. Evidence for collapsin-1 functioning in the control of neural crest migration in both trunk and hindbrain regions. Development 126, 2181–2189.

Farlie, P.G., Kerr, R., Thomas, P., Symes, T., Minichiello, J., Hearn, C.J., Newgreen, D., 1999. A paraxial exclusion zone creates patterned cranial neural crest cell outgrowth adjacent to rhombomeres 3 and 5. Dev. Biol. 213, 70–84.

Fasano, L., Roder, L., Core, N., Alexandre, E., Vola, C., Jacq, B., Kerridge, S., 1991. The gene teashirt is required for the development of *Drosophila* embryonic trunk segments and encodes a protein with widely spaced zinc finger motifs. Cell 64, 63–79.

Flanagan, J.G., Vanderhaeghen, P., 1998. The ephrins and Eph receptors in neural development. Annu. Rev. Neurosci. 21, 309–345.

Gallet, A., Angelats, C., Erkner, A., Charroux, B., Fasano, L., Kerridge, S., 1999. The C-terminal domain of armadillo binds to hypophosphorylated teashirt to modulate wingless signalling in *Drosophila*. EMBO J. 18, 2208–2217.

Golding, J.P., Trainor, P., Krumlauf, R., Gassmann, M., 2000. Defects in pathfinding by cranial neural crest cells in mice lacking the neuregulin receptor ErbB4. Nat. Cell Biol. 2, 103–109.

Helbling, P.M., Tran, C.T., Brandli, A.W., 1998. Requirement for EphA receptor signaling in the segregation of *Xenopus* third and fourth arch neural crest cells. Mech. Dev. 78, 63–79.

Hemmati-Brivanlou, A., Harland, R.M., 1989. Expression of an engrailed-related protein is induced in the anterior neural ectoderm of early *Xenopus* embryos. Development 106, 611–617.

Hemmati-Brivanlou, A., de la Torre, J.R., Holt, C., Harland, R.M., 1991. Cephalic expression and molecular characterization of *Xenopus* En-2. Development 111, 715–724.

Holder, N., Klein, R., 1999. Eph receptors and ephrins: effectors of morphogenesis. Development 126, 2033–2044.

Hollemann, T., Bellefroid, E., Pieler, T., 1998a. The *Xenopus* homologue of the *Drosophila* gene tailless has a function in early eye development. Development 125, 2425–2432.

Hollemann, T., Chen, Y., Grunz, H., Pieler, T., 1998b. Regionalized metabolic activity establishes boundaries of retinoic acid signalling. EMBO J. 17, 7361–7372.

Hollemann, T., Panitz, F., Pieler, T., 1999. In situ hybridization techniques with *Xenopus* embryos. A Comparative Methods Approach to the Study of Oocytes and Embryos. Oxford Univ. Press, Oxford, pp. 279–290.

Hopwood, N.D., Pluck, A., Gurdon, J.B., 1989. A *Xenopus* mRNA related to *Drosophila* twist is expressed in response to induction in the mesoderm and the neural crest. Cell 59, 893–903.

Hörstadius, S., Sellman, S., 1946. Experimentelle Untersuchungen über die Determination des knorpeligen Kopfskeletts bei Urodelen. Nov. Act. Reg. Societ. Scient. Upsal. Ser. IV. 13 (8), 4–170.

Hunt, P., Krumlauf, R., 1991. Deciphering the Hox code: clues to patterning branchial regions of the head. Cell 66, 1075–1078.

Hunt, P., Gulisano, M., Cook, M., Sham, M.H., Faiella, A., Wilkinson, D., Boncinelli, E., Krumlauf, R., 1991. A distinct Hox code for the branchial region of the vertebrate head. Nature 353, 861–864.

Kiecker, C., Niehrs, C., 2001. A morphogen of Wnt/β-catenin signaling regulates anteroposterior neural patterning in *Xenopus*. Development 128, 4189–4201.

Kim, S., Yamamoto, A., Bouwmeester, T., Agius, E., De Robertis, E.M., 1998. The role of Paraxial Protocadherin in selective adhesion and cell movements of the mesoderm during *Xenopus* gastrulation. Development 125, 4681–4691.

Krull, C.E., Lansford, R., Gale, N.W., Collazo, A., Marcelle, C., Yancopoulos, G.D., Fraser, S.E., Bronner-Fraser, M., 1997. Interactions of Eph-related receptors and ligands confer rostrocaudal pattern to trunk neural crest migration. Curr. Biol. 7, 571–580.

Kudoh, T., Wilson, S.W., Dawid, I.B., 2002. Distinct roles for Fgf, Wnt and retinoic acid in posteriorizing the neural ectoderm. Development 129, 4335–4346.

Lamb, T.M., Knecht, A.K., Smith, W.C., Stachel, S.E., Economides, A.N., Stahl, N., Yancopolous, G.D., Harland, R.M., 1993. Neural induction by the secreted polypeptide noggin. Science 262, 713–718.

Lumsden, A., Sprawson, N., Graham, A., 1991. Segmental origin and migration of neural crest cells in the hindbrain region of the chick embryo. Development 113, 1281–1291.

Manfroid, I., Caubit, X., Kerridge, S., Fasano, L., 2004. Three putative murine Teashirt orthologues specify trunk structures in the same way as the *Drosophila* teashirt gene. Development 131, 1065–1073.

McCormick, A., Coré, N., Kerridge, S., Scott, M.P., 1995. Homeotic response elements are tightly linked to tissue-specific elements in a transcriptional enhancer of the teashirt gene. Development 121, 2799–2812.

McGrew, L.L., Otte, A.P., Moon, R.T., 1992. Analysis of Xwnt-4 in embryos of *Xenopus laevis*: a Wnt family member expressed in the brain and floor plate. Development 115, 463–473.

Mizuseki, K., Kishi, M., Matsui, M., Nakanishi, S., Sasai, Y., 1998. *Xenopus* zic-related-1 and Sox2, two factors induced by chordin, have distinct activities in the initiation of neural induction. Development 125, 579–587.

Newman, C.S., Grow, M.W., Cleaver, O., Chia, F., Krieg, P., 1997. Xbap, a vertebrate gene related to bagpipe, is expressed in developing craniofacial structures and in anterior gut muscle. Dev. Biol. 181, 223–233.

Noden, D.M., 1993. The role of the neural crest in patterning of avian cranial skeletal, connective and muscle tissues. Dev. Biol. 96, 144–165.

Pannese, M., Polo, C., Andreazzoli, M., Vignali, R., Kablar, B., Barsacchi, G., Boncinelli, E., 1995. The *Xenopus* homologue of Otx2 is a maternal homeobox gene that demarcates and specifies anterior body regions. Development 121, 707–720.

Pasqualetti, M., Ori, M., Nardi, I., Rijli, F.M., 2000. Ectopic Hoxa2 induction after neural crest migration results in homeosis of jaw elements in *Xenopus*. Development 127, 5367–5378.

Prince, V., Lumsden, A., 1994. Hoxa-2 expression in normal and transposed rhombomeres: independent regulation in the neural tube and neural crest. Development 120, 911–923.

Rijli, F.M., Mark, M., Lakkaraju, S., Dierich, A., Dolle, P., Chambon, P., 1993. A homeotic transformation is generated in the rostral branchial region of the head by disruption of Hoxa-2, which acts as a selector gene. Cell 75, 1333–1349.

Roberts, D.J., Smith, D.M., Goff, D.J., Tabin, C.J., 1998. Epithelial–mesenchymal signaling during the regionalization of the chick gut. Development 125, 2791–2801.

Röder, L., Vola, C., Kerridge, S., 1992. The role of the teashirt gene in trunk segmental identity in *Drosophila*. Development 115, 1017–1033.

Sadaghiani, B., Thiébaud, C.H., 1987. Neural crest development in the *Xenopus*

laevis embryo, studied by interspecific transplantation and scanning electron microscopy. Dev. Biol. 124, 91–110.

Saller, E., Kelley, A., Bienz, M., 2002. The transcriptional repressor Brinker antagonizes Wingless signaling. Genes Dev. 16, 1828–1838.

Salzberg, A., Elias, S., Nachaliel, N., Bonstein, L., Henig, C., Frank, D., 1999. A Meis family protein caudalizes neural fates in *Xenopus*. Mech. Dev. 80, 3–13.

Santagati, F., Rijli, F.M., 2003. Cranial neural crest and the building of the vertebrate head. Nat. Rev., Neurosci. 4, 806–818.

Sasai, Y., Lu, B., Steinbeisser, H., Geissert, D., Gont, L.K., De Robertis, E.M., 1994. *Xenopus* chordin: a novel dorsalizing factor activated by organizer-specific homeobox genes. Cell 79, 779–790.

Sekimoto, T., Yoshinobu, K., Yoshida, M., Kuratani, S., Fujimoto, S., Araki, M., Tajima, N., Araki, K., Yamamura, K., 1998. Region-specific expression of murine Hox genes implies the Hox code-mediated patterning of the digestive tract. Genes Cells 3, 51–64.

Smith, A., Robinson, V., Patel, K., Wilkinson, D.G., 1997. The EphA4 and EphB1 receptor tyrosine kinases and ephrin-B2 ligand regulate targeted migration of branchial neural crest cells. Curr. Biol. 7, 561–570.

Trainor, P.A., Krumlauf, R., 2000a. Plasticity in mouse neural crest cells reveals a new patterning role for cranial mesoderm. Nat. Cell Biol. 2, 96–102.

Trainor, P.A., Krumlauf, R., 2000b. Patterning the cranial neural crest: hindbrain segmentation and Hox gene plasticity. Nat. Rev., Neurosci. 1, 116–124.

Trainor, P.A., Ariza-McNaughton, L., Krumlauf, R., 2002. Role of the isthmus and FGFs in resolving the paradox of neural crest plasticity and prepatterning. Science 295, 1288–1291.

Wacker, S.A., Jansen, H.J., McNulty, C.L., Houtzager, E., Durston, A.J., 2004. Timed interactions between the Hox expressing non-organiser mesoderm and the Spemann organiser generate positional information during vertebrate gastrulation. Dev. Biol. 268, 207–219.

Waltzer, L., Vandel, L., Bienz, M., 2001. Teashirt is required for transcriptional repression mediated by high Wingless levels. EMBO J. 20, 137–145.

Wang, H.U., Anderson, D.J., 1997. Eph family transmembrane ligands can mediate repulsive guidance of trunk neural crest migration and motor axon outgrowth. Neuron 18, 383–396.

Winning, R.S., Sargent, T.D., 1994. Pagliaccio, a member of the Eph family of receptor tyrosine kinase genes, has localized expression in a subset of neural crest and neural tissues in *Xenopus laevis* embryos. Mech. Dev. 46, 219–229.

Winning, R.S., Shea, L.J., Marcus, S.J., Sargent, T.D., 1991. Developmental regulation of transcription factor AP-2 during *Xenopus laevis* embryogenesis. Nucleic Acids Res. 19, 3709–3741.

Xu, Q., Alldus, G., Holder, N., Wilkinson, D.G., 1995. Expression of truncated Sek-1 receptor tyrosine kinase disrupts the segmental restriction of gene expression in the *Xenopus* and zebrafish hindbrain. Development 121, 4005–4016.

Yokota, C., Kofron, M., Zuck, M., Houston, d.W., Isaacs, H., Asashima, M., Wylie, C.C., Heasman, J., 2003. A novel role for a nodal-related protein; Xnr3 regulates convergent extension via the FGF receptor. Development 130, 2199–2212.

Zhang, J., Bai, S., Zhang, X., Nagase, H., Sarras, M.P., 2003. The expression of gelatinase A (MMP-2) is required for normal development of zebrafish embryos. Dev. Genes Evol. 213, 456–463.